ACS APPLIED POLYMER MATERIALS

pubs.acs.org/acsapm

Article

Kraft Lignin Periodate Oxidation for Biobased Wood Panel Resins

Archana Bansode, Lorena Alexandra Portilla Villarreal, Yuyang Wang, Osei Asafu-Adjaye, Brian K. Via, Ramsis Farag, Iris Beatriz Vega Erramuspe,* and Maria L. Auad

Cite This: *ACS Appl. Polym. Mater.* 2023, 5, 4118−4126

Read Online

ACCESS | Metrics & More | Article Recommendations | Supporting Information

ABSTRACT: The development of biobased resins with high-bonding performance has gained considerable attention in the wood industry. In this study, we developed biobased novolacs phenol-formaldehyde (BNPF) resins by partially replacing petroleum-based phenol and formaldehyde with lignin derived from kraft biorefinery and modified kraft biorefinery-derived lignin, respectively. We first performed a mild and efficient chemical modification of the lignin through the periodate oxidation process. Sodium periodate was used to oxidize the hydroxyl functional groups present in the interunit linkages (β-O-4 bond) in the lignin structure and convert lignin partly to quinones. This was assessed by Fourier-transform infrared spectroscopy, elemental analysis, solid-state $^{1}H-^{13}C$ 2D HETCOR NMR, and aldehyde content analysis. We synthesized a series of BNPF resins by replacing phenol with lignin, then by replacing formaldehyde with oxidized lignin, and finally by replacing both phenol and formaldehyde with lignin and oxidized lignin. The structural characterization results of the NPF resins revealed the formation of methylene linkages in the phenolic rings. Before application as wood adhesives, we studied the curing behavior of the formulated adhesive via differential scanning calorimetry. The adhesion strength of the adhesive was determined using the tensile shear strength analysis. The bonding performance tests indicated that BNPF resin adhesives have high adhesion strengths (>0.7 MPa). The outcome of this research provides a promising perspective to utilize natural polymers such as lignin for the synthesis of biobased wood adhesives.

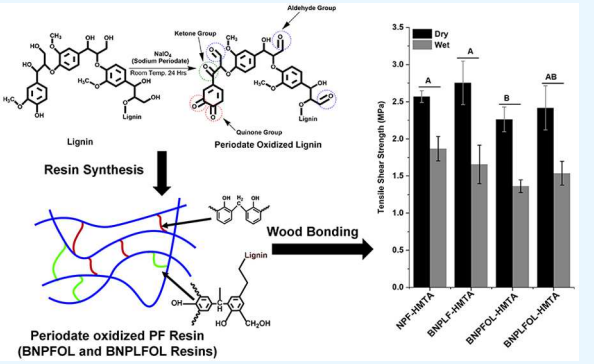

KEYWORDS: *lignin, periodate oxidation, oxidized lignin, characterization, phenol-formaldehyde resin, wood adhesive*

INTRODUCTION

Engineered wood-based panels show a wide range of applications in internal wall partitioning, sheathing, roofing, ceilings, furniture, and structural insulated panels. This is due to their design flexibility, durability, strength, and cost-effectiveness.[1,2] Laminated veneer lumber, plywood, particle boards, medium density boards (MDFs), and oriented strand board (OSB) mainly used wood-based panels (WBPs).[3,4] In addition, wood adhesives have contributed to the fabrication and preparation of WBPs, which account for nearly 65% of the total world adhesives.[5−7] Various wood adhesives on the market are thermoplastics and thermoset resins, such as phenol-formaldehyde (PF), melamine-formaldehyde (MF), urea-formaldehyde (UF), polyurethane, and polymeric methylene diphenyl diisocyanate (pMDI).[8,9] Moreover, most of these resins are aldehyde-based adhesives, dominating the wood adhesive industry due to their high adhesion strength and low cost.[10] Among them, PF resins are predominantly used due to the widespread availability of phenol and formaldehyde.[11,12] Depending on the structure and curing process, the PF resins are classified as resol-type PF resin or novolac-type PF resin. Resole-type PF resin is produced by the polycondensation reaction of phenol with the molar excess of formaldehyde (P/F molar ratio of 1:1.1 or more) under an alkaline catalyst. In contrast, the reaction of excess phenol with formaldehyde (P/F molar ratio 1:0.75 or less) in acidic conditions yields novolacs.[13−15]

However, the formation of these resins still relies on nonrenewable petrochemicals such as phenol and formaldehyde, which would release formaldehyde and other toxic substances in high concentrations that are hazardous to humans and pollute the environment during production and use.[16] Thus, extensive research is being conducted in academia and industry for replacing phenol and formaldehyde with potential biobased renewable resources to produce more environmentally friendly wood adhesives.[14,17]

Within this context, lignin has gained significant interest as a promising sustainable alternative for replacing phenol in PF resin due to their structural similarities of having active H from the aromatic hydroxyl-containing group (Ar−OH).[17] Lignin is

Received: February 18, 2023
Accepted: May 3, 2023
Published: May 22, 2023

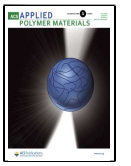

https://doi.org/10.1021/acsapm.3c00324
ACS Appl. Polym. Mater. 2023, 5, 4118−4126

one of the three polymers of lignocellulosic biomass, which is primarily composed of cellulose, hemicellulose, and lignin. Lignin is distributed throughout the secondary cell wall of plants that provides strength and rigidity to the secondary cell walls. This polyphenolic and amorphous macromolecule is the second most abundant resource after cellulose, and it is formed through radical polymerization of phenylpropane units: *p*-hydroxyphenyl (H), guaiacyl (G), and syringyl (S). The monomeric units H, G, and S are randomly linked through different linkages, including *β*-O-4, *β*-*β*, and *β*-5 covalent bonds, depending upon the botanic origin and extraction process, resulting in versatile functionality.[18,19] In the pulp and paper mills, lignin is generated as a waste byproduct (black liquor) during the delignification of the lignocellulosic biomass by immersing it in an aqueous solution with alkaline chemicals at elevated temperatures (cooking).[20] However, the lignin-containing black liquor, which is separated from the fibrous material after the cooking process, is underutilized and usually burned for energy production and heat.[21] To this end, some processes are employed to recover lignin from black liquor. In this respect, Ingevity (formerly known as Westvaco) recovers lignin (marketed as INDULIN trademark) from black liquor.[22] Also, an industrial kraft lignin marketed by Stora Enso (Finland) under the name Lineo used as a sustainable alternative for replacing various phenol-based resins and oil-based binders in asphalt.[23]

In recent decades, numerous research studies have been reported on exploiting lignin as a phenol replacement in PF resin synthesis for wood adhesive applications.[17,20,24−30] In our prior work, we successfully used kraft lignin (Indulin AT from Ingevity) as a partial replacement for phenolic monomer synthesis of biobased Novolac PF (BNPF) resin for wood bonding. The work showed that synthesized lignin-based PF resin exhibited the highest adhesion strength compared to the standard Novolac PF resin (NPF).[31] Despite these achievements in reducing phenol consumption in PF resin synthesis, using the second primary ingredient, i.e., formaldehyde, has remained a significant concern due to its high toxicity.[32] Hence, to further enhance the sustainability of the PF resin and broaden the utilization of lignin, the substitution of formaldehyde with a chemical modification of lignin has become an exciting area of research to explore different strategies.[33]

Among the various chemical modification routes, oxidation is a promising technique that selectively cleaves the chemical bonds and allows the addition of new functionalities (i.e., aldehydes and carboxylate groups). In this regard, periodate oxidation processes have been reported where highly reactive aldehyde groups are introduced into the structure by oxidizing the hydroxyl groups. In the past, the cellulose is subjected to a reaction with the sodium periodate ($NaIO_4$), leading to a highly oxidized form of dialdehyde cellulose (DAC) through oxidation on C2 and C3 positions of the anhydroglucose units.[8,34,35] Considering the diversity of functional groups, specific oxidation of lignin has been carried out under mild conditions. Therein, *β*-O-4 linkages present in the lignin are selectively cleaved by a periodate oxidant, thereby adding aldehyde functionality to the lignin structure.[36] Zhang and Fatehi[37] reported a two-step periodate oxidation of carbohydrate-enriched hydrolysis lignin leading to the formation of muconic functional groups in the lignin structure. Further, the periodate oxidized network can react with the hydroxyl and activates reactive phenolic sites during respective synthesis to yield environmental friendly biobased wood adhesives.[36,38]

Herein, this work intends to develop more sustainable PF resin wood adhesives. We describe the oxidation of hydroxyl vicinal to *β*-O-4 bonds in the lignin structure using sodium periodate ($NaIO_4$) as an oxidizing agent under mild conditions. To better understand the chemical structure of the oxidized lignin (OL), FTIR, elemental analysis, aldehyde content, and solid-state $^{1}H-^{13}C$ 2D HETCOR NMR techniques were used to investigate the structural features. A series of BNPF resins were synthesized by first replacing phenol with lignin (BNPLF), then by replacing formaldehyde with OL (BNPFOL), and later by replacing both phenol and formaldehyde with lignin and OL (BNPLFOL), respectively. The prepared resin adhesive was applied on the wood substrate, and respective adhesion strength was measured.

EXPERIMENTAL SECTION

Materials. Indulin AT lignin (softwood) from a kraft pulping process was generously supplied by Ingevity Corporation, South Carolina. Phenol (99%), formalin solution (37% formaldehyde in water), ethanol (200 proof), methanol (99.8%), sulfuric acid (H_2SO_4; 95.0−98.0%), deuterated dimethyl sulfoxide (DMSO-d_6, 99.9%), and hexamethylenetetramine (HMTA, 99+%) were supplied by VWR International, USA. Sodium periodate ($NaIO_4$, 99.0%) was purchased from Acros Organics, USA. 2,4-dinitrophenylhydrazine (DNPH) and oxalic acid (anhydrous crystal, 98.0%) were acquired from Spectrum Chemical Manufacturing Corporation, USA.

Periodate Oxidation of Lignin. The periodate oxidation has been performed to introduce the aldehyde groups in the lignin by oxidizing the hydroxyl groups. Briefly, for each batch of periodate OL, 20 g of kraft Indulin AT lignin (L) was mixed with the 50 g $NaIO_4$ and added to the 500 mL ethanol (15%). Further, this mixture was loaded into the pressure-resistant bottle and wrapped with a layer of aluminum foil to prevent the decomposition of $NaIO_4$ by exposure to light. The reaction was carried out under mild stirring at room temperature allowing the oxidation to proceed overnight (or for 24 h). The product was then purified using methanol by centrifuging and decanting at least three times. After that, the product was dried at 40 °C in a vacuum oven.

Structural Characterization of Periodate OL. *Fourier-Transform Infrared (FTIR) Spectroscopy.* FTIR analysis of Indulin AT lignin (L) and periodate OL was carried out on the Nicolet 6700 FTIR spectrophotometer (Thermo Fisher Scientific Instrument., USA) equipped with attenuated total reflectance (ATR) accessory containing a diamond crystal. The spectrum was collected in the transmission mode over a region of 4000−600 cm^{-1} using 64 scans at a resolution of 4 cm^{-1}. Before every sampling, the background spectrum was collected. The software used for FTIR evaluation was OMNIC Version 7.3.

Elemental Analysis. Elemental analysis (C, H, and N) of Indulin AT L and periodate OL was performed in a Flash 2000 Elemental Analyzer (Thermo Fisher Scientific, Bremen, Germany) operating with the dynamic flash combustion of the samples. The aspartic acid weight used as a standard was 3.00−4.00 mg, and the weight of the unknown samples. All samples were weighed in aluminum tin capsules and dropped into the combustion reactor (left furnace) from the Thermo Scientific MAS Plus Autosampler. The samples were combusted in the reactor initially set at 950 °C in oxygen and helium (carrier gas). The elemental gases were carried out into the gas chromatography column set at 75 °C and detected in a highly sensitive thermal conductivity detector (TCD) set at 1000 *μ*V. The collected data were analyzed using Eager Xperience for flash elemental analyzers software (EA111X F/W Ver. 1.12, EA111x OCX Ver. 01.02). All the samples were analyzed in three replicate specimens. The results were reported as averaged values in percent by weight.

Determination of Aldehyde Content. In the analysis of aldehyde groups, often 2,4-dinitrophenylhydrazine (DNPH) reagent is used, and the subsequent reagent solution was prepared using the procedure in the literature.[39−41] Briefly, 143 mg of DNPH has

https://doi.org/10.1021/acsapm.3c00324
ACS Appl. Polym. Mater. 2023, 5, 4118−4126

dissolved in 15 mL of concentrated sulfuric acid in 500 mL of a volumetric flask, and then 156.25 mL of ethanol (96%) in this mixture, and the final volume was made up to the mark with distilled water. Later, the solution was placed in the ultrasonic bath for 15 min to achieve a homogenized solution. Alternatively, a blank solution was prepared with the same procedure except for adding the DNPH reagent. A series of standard solutions 20, 40, 60, 80, and 100 mg/mL were prepared using the DNPH reagent solution to generate a calibration curve. After that, the quantitative aldehyde analysis of Indulin AT lignin (L) and periodate OL was performed by weighing 30 mg of sample in 10 mL of the centrifuge tube, followed by the addition of 10 mL freshly prepared DNPH reagent solution. The subsequent reactive mixture was centrifuged for 10 min using 4200 rpm. Finally, the aldehyde content was investigated by measuring absorbance with a Genesys 150 UV−Visible spectrophotometer in the range of 200−800 nm using a blank solution as background. The amount of aldehyde generated was calculated using eq 1.[39]

$$\text{Aldehyde concentration (mmol/g)} = \frac{\frac{\text{Reacted DNPH (mmol / g)}}{198.14}}{\text{Concentration (\%)} \times 10^{-4}} \quad (1)$$

where 198.14 is the molecular weight of DNPH.

Solid-State Two-Dimensional Heteronuclear Correlation Nuclear Magnetic Resonance (ss ^{1}H−^{13}C 2D HETCOR NMR). Solid-state ^{1}H−^{13}C 2D HETCOR NMR experiment of Indulin AT lignin (L) and periodate OL was performed in the Bruker AVIII-HD 500 nuclear magnetic resonance (NMR) spectrometer equipped with standard Bruker 3.2 mm CP-MAS at Magnetic Resonance Imaging Core Facility at Georgia Institute of Technology, Atlanta. The combination of cross-polarization (CP) with magic angle spinning (MAS) is commonly used to perform solid-state NMR. The HETCOR measurements were recorded using "lghetfq" pulse program from the Bruker library for homonuclear decoupling of ^{1}H. All the spectra ran with a contact time of 2 ms under CP conditions, and the spinning speed was set to 14.0 kHz. The total experimental time for each sample is 12.34 h. The initial spectral processing was done using Bruker's Topspin 3.2 software, and structure analysis was done later using Mestrelab Research (MestReNova Version 7.1.1) software.

Synthesis and Characterization of Biobased NPF Resins (BNPF). The acid-catalyzed condensation reaction between phenol and formaldehyde for the synthesis of a Novolac PF (NPF) resin was carried out following the procedure reported in the previously published article.[31] Briefly, phenol (94 g, 1.0 mol) and oxalic acid (4.7 g, 0.05 mol) were added into a 500 mL four-necked round bottom flask. Later, the flask equipped with a mechanical stirrer, condenser, and dropping funnel was placed in a silicone oil bath under magnetic stirring. First, the reaction mixture was heated to 90 °C, and then 37% formalin solution (64.87 g, 0.8 mol of formaldehyde: 24 g) was slowly added to this mixture through an attached funnel dropwise. After the complete addition of formaldehyde, the reaction continued for 3 h at 90 °C. Once the reaction was completed, the reaction product was cooled down to room temperature and washed to remove the unreacted reaction component with distilled water (DI), followed by freeze-drying. Furthermore, three different biobased-NPF resins (BNPF) were prepared according to the recipe reported in Table 1 by following the same reaction conditions described above. Finally, the prepared NPF and BNPF resins were characterized using FTIR and ^{13}C−^{1}H HSQC 2D-NMR techniques.

Solution-State Two-Dimensional Heteronuclear Single Quantum Coherence NMR (Solution-State ^{1}H−^{13}C 2D HSQC NMR) Analysis. NPF and BNPF resins were thoroughly identified by the solution-state ^{1}H−^{13}C 2D HSQC NMR analysis technique. The NMR spectra were recorded using hsqctgpsisp 2.2. pulse program on the Bruker Ultrashield Plus 500 MHz spectrometer with a broadband nitrogen-cooled prodigy probe. For each NMR experiment, approximately 155 mg of the sample was dissolved entirely in 1000 μL DMSO-d_6 solvent. The mixture was transferred into 5 mm NMR tubes, and the experiment was performed with the following parameters: spectral width from 0 to 13 ppm in the F2 (^{1}H) with 1024 data points (TD1) and spectral width from 0 to 220 ppm in F1 (^{13}C) with 256 data points (TD2), 90° pulse angle, a pulse delay of 1.5 s, $^{1}J_{CH}$ used was 145 Hz, an acquisition time of 0.11 s, scan number of 16, and dummy scan number of 16. The chemical shifts were referenced to the central solvent DMSO-d_6 peak (δ = 2.49 ppm) and δ = 39.5 ppm) for ^{1}H NMR and ^{13}C NMR, respectively. The NMR data were analyzed using Mestrelab Research software (MestReNova Version 7.1.1).

Table 1. Reaction Recipe of Acid-Catalyzed Condensation Polymerization Reaction of Four NPF Resins and Their Designations ((*) BNPF Resins)

	phenolic monomer		aldehyde monomer	
resin samples	phenol (g)	lignin (g)	formaldehyde (g)	oxidized lignin (g)
NPF	94		24	
PLF*	49	49	24	
PFOL*	94		12	12
PLFOL*	49	49	12	12

Thermal Study of NPF and BNPF Resins by Differential Scanning Calorimetry (DSC). The prepared NPF and BNPF resins were further reacted with the HMTA curing agent, which generates in situ reactive methylene carbocations and compensates for the deficiency of formaldehyde in the NPF resin. The addition of HMTA DSC was performed on TA Instruments (TA Q2000, DE, and USA) to determine the peak exothermic temperature associated with the curing process. For DSC analysis, each resin sample was grounded with the HMTA curing agent (9% w/w HMTA/NPF resin) using mortar and pestle, yielding four wood adhesive mixtures: NPF-HMTA Resin, BNPLF-HMTA Resin, BNPFOL-HMTA Resin, and BNPLFOL-HMTA Resin. Next, about 5−6 mg of the subsequent adhesive was loaded into the DSC standard aluminum pans and sealed with DSC standard aluminum lid, and then heated from 25 to 200 °C at a rate of 10 °C/min under a nitrogen atmosphere with a flow rate of 50 mL/min. The generated curing thermograms were analyzed using TA instrument analysis software.

Preparation of Different PF Resin-Glued Wood Specimens. All the biobased PF resins adhesion testing was conducted on southern yellow pine (SYP) wood specimens cut into a size of 320 × 46 × 10.5 mm^3 ($L \times W \times H$), which have been widely used for adhesive testing. After being conditioned at a relative humidity of (65 ± 5%) and at 22 ± 2 °C for 7 days, the biobased PF resin was spread with an adhesive content of about 200 g/m^2 on the single side of the veneer, and then the uncoated veneer was overlapped on the coated veneer by applying light pressure manually. Subsequently, assembled wood strips were hot-pressed at 200 °C for 5 min with the applied pressure of 2 MPa. After hot pressing, the glued wood specimens were cooled down and maintained for 24 h to release internal stress before cutting them into the desired size. Eight specimens per bonded adhesives were cut and from this group of cut eight wood specimens, four samples were chosen for the dry bonding strength, and the remaining samples were submersion in water at room temperature for 24 h to perform the wet bonding strength followed by air drying of wood specimens for 15 min.

Characterization of the PF Resin-Glued Wood Specimens. *Tensile Shear Strength.* The biobased PF adhesives bonded wood specimens were tested at a speed of 1.0 mm/mm on an Instron 5900 Universal Material Testing Instrument (Bluehill, Instron, MA, USA) attached with a 100 kN load cell, and the collected data were processed using a Bluhill 3.0 software. The tensile shear strength was calculated using eq 2.

$$\tau = \frac{F}{A} \quad (2)$$

where τ is the tensile shear strength (N/mm^2 or MPa), F is the maximum force to break the adhesive (N), and A is the shear area (mm^2).

https://doi.org/10.1021/acsapm.3c00324
ACS Appl. Polym. Mater. 2023, 5, 4118−4126

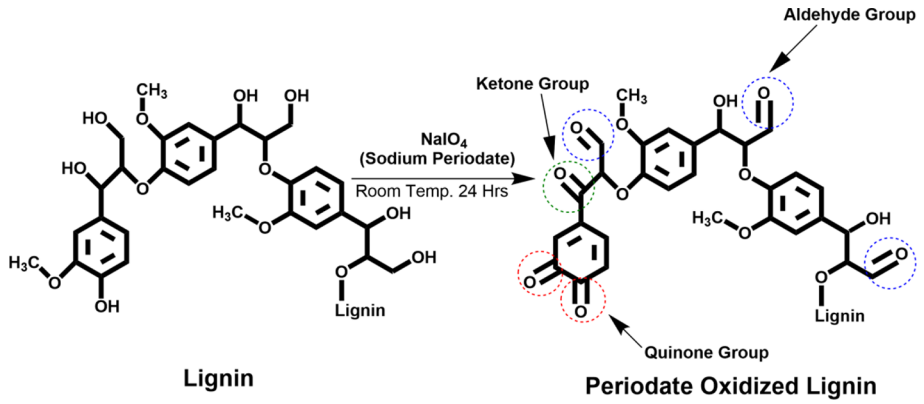

Figure 1. Oxidation of guiacyl units and primary and secondary alcohols in softwood lignin during the periodate oxidation reaction.

The tensile shear strength, water absorption, and thickness swelling data of the NPF and BNPF resins were measured in quartets and expressed as the mean value ± the corresponding standard deviation (SD) value. Further, data were subjected to using two-way analysis of variance (ANOVA) with Tukey's post-hoc test for statistical significance analysis. The statistical analysis was carried out using Minitab 19 software.

RESULTS AND DISCUSSION

Characterization of Periodate Oxidized Lignin. The structure of the Indulin AT lignin after periodate oxidation was evaluated by various analytical techniques, including FTIR, elemental analysis, $^{1}H-^{13}C$ 2D HETCOR NMR technique, and aldehyde content and further compared with the unmodified lignin. Figure 1 illustrates the quinone, ketone, and aldehyde groups formed during the oxidation reaction with periodate. However, it should be noted that this structure does not accurately represent the real structure of OL because it does not account for all the groups modified during the experiment.

The FTIR-ATR analysis first examined the influence of periodate oxidation on the lignin structure, and the spectra are shown in Figure 2. The two peaks at 2935 and 2840 cm^{-1} belong to the methoxy group linked to the C−H stretching (Figure 2a). In the OL structure (Figure 2b), the band intensity of the C−H stretching decreased at 2935 and 2840 cm^{-1}, indicating the removal of the methoxy group from the aromatic lignin ring. The increased intensity of peaks at 1733 cm^{-1} highlighted the introduction of the carbonyl (C═O) group (aldehyde) that is formed during the oxidation of hydroxyl groups present in the interunit linkages (β-O-4 bond) in the lignin structure. A new peak observed in Figure 2b at 1630 cm^{-1} highlighted the presence of the quinone group. A similar observation was reported in the literature with the periodate oxidation of softwood lignin.[38] The peaks around 1509, 1450, and 1425 cm^{-1} were attributed to aromatic skeleton vibrations. The absorption bands at 1218, 1125, and 1029 cm^{-1} were due to the C−O stretching vibration deriving from the guaiacyl ring, and secondary and primary alcohols (C−OH), respectively, which weakened in intensity after undergoing oxidation. The peaks detected in the region 1000−750 cm^{-1} were assigned to the aromatic C−H out-of-plane deformations. The characteristic peaks associated with lignin detected were also observed in the FTIR-ATR spectrum of OL, indicating that there are limited changes in the lignin chemical structure after oxidation.

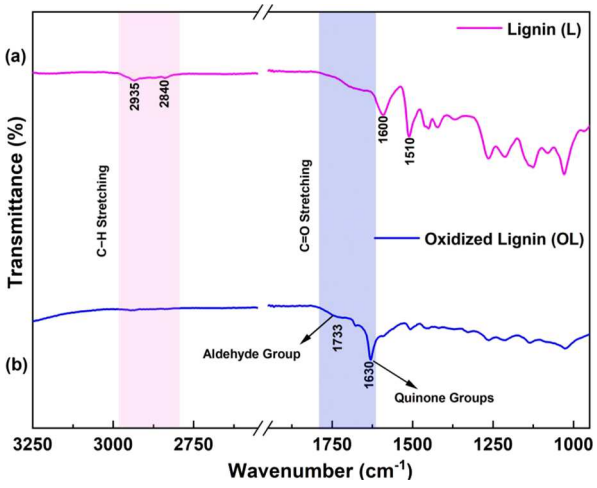

Figure 2. FTIR spectra of (a) lignin (L) and (b) periodate oxidized lignin (OL).

The elemental compositions (C, H, and O) of the lignin and OL were determined and are reported in Table 2. A relatively smaller amount of nitrogen element was detected in the plant resource-based lignin. The contents of carbon (59.80−21.56%) and hydrogen (5.71−2.60%) decreased. Still, oxygen content increased from 34.08 to 75.79% in OL compared to the lignin due to the oxidation hydroxyl groups present in the interunit linkages (β-O-4 bond) in the lignin structure and partial conversion of lignin to quinone groups.

The synthesized OL was partially soluble in the desired NMR solvents compared with the lignin as the molecular weight of the lignin increases after the periodate oxidation process.[37] In this respect, the solid-state $^{1}H-^{13}C$ 2D HETCOR NMR technique is considered an advantageous method for elucidating the structure of lignin, which is not limited by its insolubility. To gain insights into the oxidative transformations of lignin, a 2D HETCOR NMR experiment was performed, as shown in Figure 3a,b. Further, the corresponding peak assignments are carried out by the following literature.[42,43] According to the 2D HETCOR, the peaks representing the aromatic carbon ($\delta C/\delta H$ 110−122/6.3−6.9 ppm) are relatively reduced in intensity in the case of OL, which could be due to the low availability of protons for the cross-polarization of aromatic carbons.[44] During the periodate oxidation, hydroxyl functional groups in the ligninare oxidized into carbonyl group. Herein, we hypothesized that the oxidation is expected to occur at hydroxyl groups attached to

https://doi.org/10.1021/acsapm.3c00324
ACS Appl. Polym. Mater. 2023, 5, 4118−4126

Table 2. Elemental Compositions of Lignin and Oxidized Lignin

samples	elemental composition (wt %)			atomic ratio		
	C %	H %	N%	O/C	H/C	O/H
lignin	59.80 ± 0.06	5.71 ± 0.01	0.39 ± 0.005	0.43	1.15	0.37
oxidized lignin	21.56 ± 0.12	2.60 ± 0.038	0.05 ± 0.020	2.63	1.44	1.82

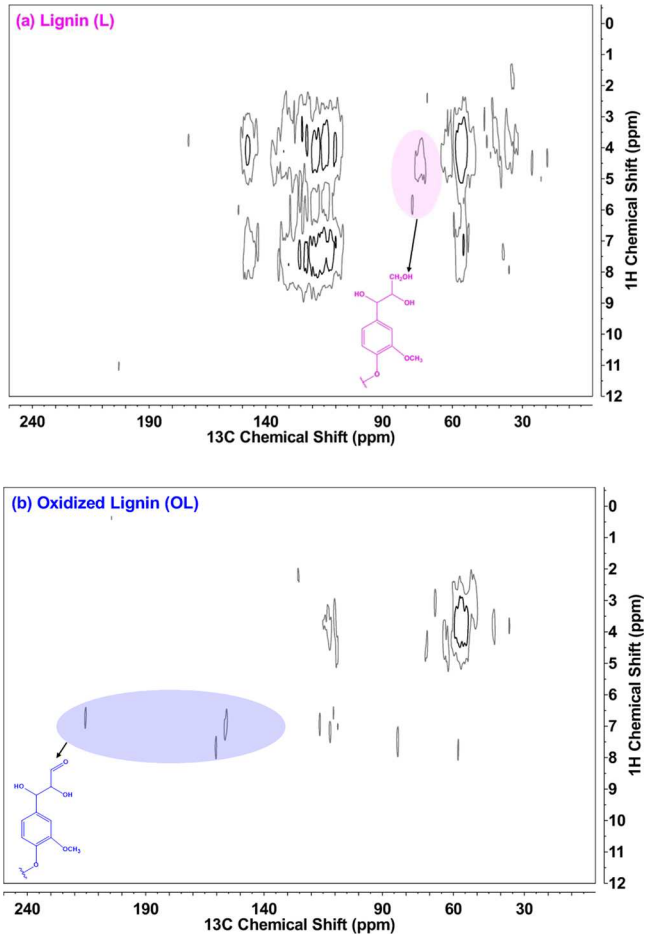

Figure 3. Solid-state $^{1}H-^{13}C$ 2D HETCOR NMR spectra of (a) lignin (L) and (b) oxidized lignin (OL).

the β-O-4 bond in the lignin, which can be confirmed by the disappearance of the peaks related to the hydroxyl groups (δC/δH 74.61−77.20/4.57−5.84 ppm) in β-O-4 linkages (Figure 3b).

Additionally, the emergence of the cross signals at 215 ppm (δC) and above ~153 ppm in Figure 4b clearly demonstrated the presence of oxidized carbon in the structure. The same cannot be seen in the lignin, Figure 3a. However, the methoxyl groups in the lignin remained unaffected since the oxidized HETCOR spectrum reveals no signals related to the quinones groups (δC 183 ppm).

In the current study, a UV−Vis-based analytical approach was applied by derivatization with 2,4-dinitrophenylhydrazine (DNPH) to investigate the possibility of the formation of aldehyde groups in the lignin structure after periodate oxidation. DNPH is the most efficient derivatization reagent that has been used extensively for aldehyde. The aldehyde content was calculated based on the calibration curve, Figure S1a,b, generated using different concentrations of the DNPH reagent solutions (20, 40, 60, 80, and 100 mg/mL), where a

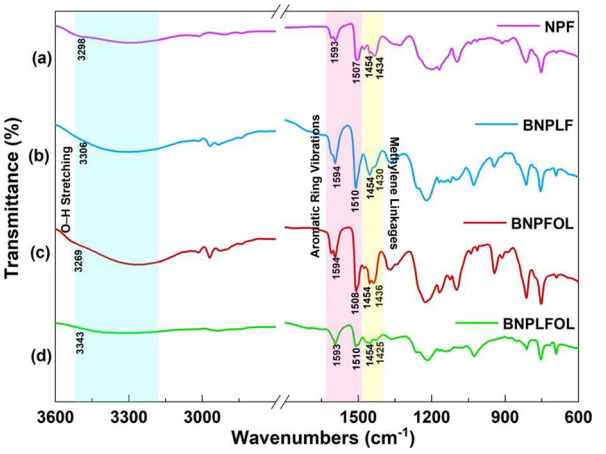

Figure 4. FTIR spectra of (a) NPF, (b) BNPLF, (c) BNPFOL, and (d) BNPLFOL.

strong UV band is attributed to the excited resonance state of the DNPH in solution. Subsequently, the lignin and OL samples were reacted with the DNPH solution, respectively. During this reaction, nucleophilic addition of the $-NH_2$ group to the carbonyl groups takes place, which results in the formation of the yellow precipitate. The UV−vis spectra of the supernatant from the DNPH-reacted lignin and oxidized sample solutions are presented in Figure S1c. The result demonstrates a distinct shift in the absorption maximum for DNPH, which is an unreacted DNPH present in the supernatant after the reaction with an aldehyde in the lignin and OL, respectively.

Furthermore, the lignin structure observed an increase in the aldehyde content from 0.0200 to 0.1116 mmol/g after oxidation treatment as reported in Table 3. Therefore, it

Table 3. Aldehyde Content of Lignin and Oxidized Lignin

	samples			
	lignin		oxidized lignin	
aldehyde content (mmol/g)	0.0200	0.00073	0.1116	0.00038

could be seen that periodate oxidation treatment introduces the aldehyde functionality in the lignin structure. During the periodate oxidation, the hydroxyl groups at the interunit linkages (β-O-4 bond) transformed into aldehyde groups, while lignin methoxy groups converted to a quinone.

Synthesis and Characterization of NPF and BNPF Resins. The NPF and BNPF resins were synthesized by forming the methylene bridges through the reaction between OH-groups of phenol and formaldehyde (CH_2O) under the acid-catalyzed process. Further, the structures of the NPF and BNPF resins were examined using FTIR and $^{13}C-^{1}H$ HSQC 2D NMR analysis techniques.

The FTIR spectra of the NPF and BNPF resins are demonstrated in Figure 4. The peaks were assigned to the corresponding functional groups based on the previous

https://doi.org/10.1021/acsapm.3c00324
ACS Appl. Polym. Mater. 2023, 5, 4118−4126

findings.[45,46] The FTIR spectra (Figure 4a–d) show the −OH bending and stretching vibrations peaks around 3500–3300 cm^{-1} regions. The peak at ∼1594 and 1510 cm^{-1} correspond to C═C stretching vibration of the aromatic ring. The signals in the region 1460–1420 cm^{-1} attributed to the methylene ($-CH_2-$) stretching vibrations after the successful addition of formaldehyde on the phenolic rings. The FTIR spectra of the BNPF resins show relatively different intensity peaks in the regions 917–912, 855–820, and 794–753 cm^{-1} which are associated with para and ortho position addition in the phenolic units, respectively.

To further understand the chemical structure, NPF and BNPF resins were characterized by the $^{13}C-^{1}H$ HSQC 2D NMR analysis experiment, and the spectra are shown in Figure 5. The obtained HSQC spectra revealed the presence of a series of characteristic peaks related to methylene bridges (Ar–CH_2–Ar) in the region (δC/δH 28.5–41.5/3.5–4.5 ppm), which originated from the acid-catalyzed condensation polymerization reaction between phenolate moieties and aldehyde functionality. Each of the NPF and BNPF resins shows peaks related to the ortho-ortho methylene linkages ($o-o'$) in the region (δC/δH 29.5/3.75 ppm), ortho-para methylene linkages ($o-p'$) in the region (δC/δH 34.3/3.75 ppm) and para-para methylene linkages ($p-p'$) in the region (δC/δH 29.5/3.75 ppm), respectively. Overall, the 2D HSQC characterization indicates that BNPF resin structures were significantly different from standard NPF resin.

Thermal Study of NPF and BNPF Resins by DSC. In the wood processing industries, evaluation of the curing temperature of the adhesive is crucial to obtain adequate curing temperature for heat pressing of wood panels. DSC analysis was used to determine the curing temperature of the adhesive. The DSC thermograms of four synthesized NPF and BNPF resins are reported in Figure 6. It can be seen that all the resins showed curing peak temperature fall in the range of 130–160 °C. A broad and intense exothermic peak occurred due to the heat generated during the polymerization reaction between reactive sites in phenol and formaldehyde. The results turned out that the NPF and BNPF resins have different reactivities, from which it can be concluded that with the replacement of both phenol and formaldehyde by lignin and OL, respectively, the curing peak temperature was shifted to a higher temperature (159.37 °C). This could be assigned to the lower reactivity of lignin and OL than phenol and formaldehyde. The partial replacement of phenol by lignin (BNPLF) or formaldehyde by OL (BNPFOL), shifted the exotherm to a lower temperature. This reduction could be beneficial to save energy consumed for the curing process of the resin.

For our study, wood panels glued with all NPF and BNPF adhesives were hot pressed at 200 °C to ensure the adhesion performance comparison performed under identical conditions.

NPF and BNPF Resin Adhesive Bonding Performance. The adhesion ability of the NPF and BNPF resins on wood specimens was evaluated by the tensile shear strength, which is defined as the adhesion strength required to rupture the bonds between the wood strands bonded by resin. The adhesion shear strength (dry and wet) of each adhesive resin is presented in Figure 7. For comparison purposes, we duplicated the BNPLF resin adhesive used in our previous work[31] and prepared it by replacing 50% (w/w) phenol with lignin and the control resin (NPF or 100% PF resin). In this study, among all

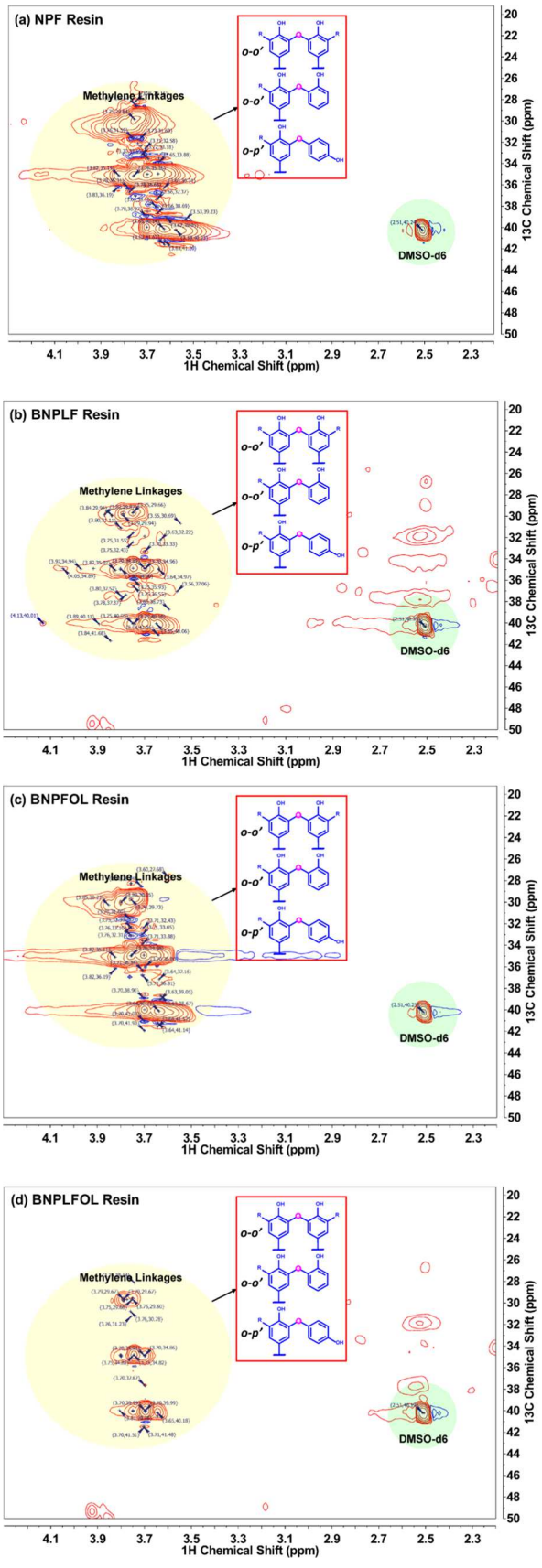

Figure 5. $^{13}C-^{1}H$ HSQC 2D-NMR spectra of (a) NPF, (b) BNPLF, (c) BNPFOL, and (d) BNPLFOL.

https://doi.org/10.1021/acsapm.3c00324
ACS Appl. Polym. Mater. 2023, 5, 4118–4126

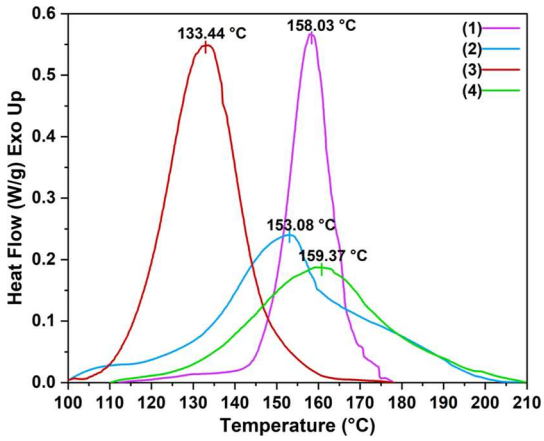

Figure 6. DSC thermograms of NPF-HMTA (1), BNPLF-HMTA (2), BNPFOL-HMTA (3), and BNPLFOL-HMTA (4). NPF, novolac phenol-formaldehyde; BNPF, biobased novolac phenol-formaldehyde; L, lignin; OL, oxidized lignin; HMTA, hexamethyelentrtramine.

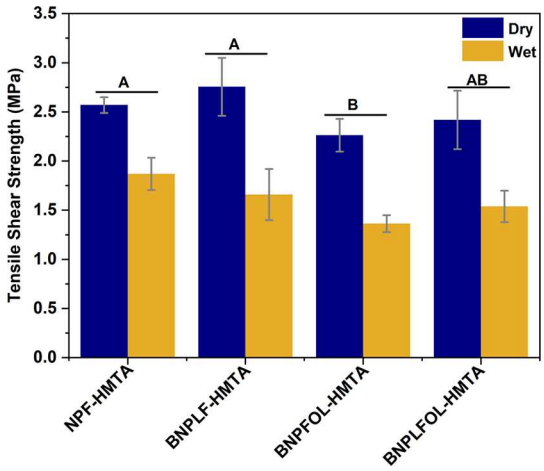

Figure 7. Dry and wet shear bonding strength of the wood specimens bonded with different adhesives: NPF-HMTA Resin, BNPLF-HMTA Resin, BNPFOL-HMTA Resin, and BNPLFOL-HMTA Resins. Letters A and B indicate mean values with statistically different adhesion strengths. NPF, novolac phenol-formaldehyde; BNPF, biobased novolac phenol-formaldehyde; L, lignin; OL, oxidized lignin; HMTA, hexamethyelentrtramine.

the tested adhesives, BNPLF-HMTA resin adhesive showed the highest dry shear strength (2.75 MPa). This suggests that replacing phenolic moieties with lignin would be beneficial.

In contrast, the pairwise comparisons using the Tukey method indicate that the adhesion strength was statistically different for the resin prepared by replacing formaldehyde with OL (BNPFOL-HMTA). A possible explanation for this could be that during BNPFOL-HMTA resin synthesis, the hydroxyl groups of the phenols could not form stronger covalent interactions with the aldehyde groups of the OL structure due to the increasing amount of the reactive sites and steric hindrance. Furthermore, the BNPLFOL-HMTA resin adhesive performed better than the BNPFOL-HMTA, owing to the growing number of polar groups which could trigger solid intermolecular interactions.

To further illustrate the versatility of the prepared BNPF resins for wood adhesive applications, the adhesion performance in a wet environment (wet shear strength) was studied. The pairwise comparisons using the Tukey method indicate that the adhesive strength of the wood panels was relatively reduced (NPF-HMTA: 2.57−1.87 MPa, BNPLF-HMTA: 2.76 to 1.66, BNPFOL-HMTA: 2.26−1.3 MPa, and BNPLFOL-HMTA: 2.42−1.54 MPa) after soaking in water for 24 h, this would be because in the humid environment, the hydrogen bonds formed between the wood surface and adhesion layer are easy to break. Whereas, in the case of BNPF resins, wet strength is drastically decreased ($p < 0.05$, Figure 7). This is because lignin has hydroxyl groups in its structure.

Overall, the bonded wood panels' dry and wet bonding strength showed their acceptable tensile shear strength, as specified by the GB/T 14732−2006 National standard (>0.7 MPa),[20] which shows the potential of the BNPF resins as wood adhesives.

CONCLUSIONS

This study presented the simultaneous replacement of both petroleum-derived phenol and formaldehyde with unfunctionalized lignin and functionalized lignin, respectively. The functionalization by periodate oxidation introduces aldehyde groups into the lignin and converts lignin partly to quinones. The dry and wet adhesion strengths of newly formulated adhesives (BNPFOL and BNPLFOL resins) were comparable to both lignin-formaldehyde resin (BNPLF) and commercially available PF resin (NPF). The replacement of formaldehyde by OL (BNPFOL) reduced the curing temperature due to the high reactivity of periodate OL compared to formaldehyde with phenol or lignin. Overall, the newly prepared BNPF adhesives in this study could be effectively used as a green alternative for the NPF resin adhesives in developing environmentally friendly wood-based panels.

ASSOCIATED CONTENT

Supporting Information

The Supporting Information is available free of charge at https://pubs.acs.org/doi/10.1021/acsapm.3c00324.

Aldehyde content measurement, (a) ultraviolet−visible spectra of different concentrations of DNPH, (b) ultraviolet-visible calibration curve of DNPH, (c) ultraviolet−visible spectra of lignin and oxidized lignin, ^{31}P NMR spectra and signal assignments of lignin, and solubility of lignin and oxidized lignin (PDF)

AUTHOR INFORMATION

Corresponding Author

Iris Beatriz Vega Erramuspe − *Forest Products Development Center, School of Forestry and Wildlife Science, Auburn University, Auburn, Alabama 36849, United States;* orcid.org/0000-0003-3347-685X; Email: ibv0002@auburn.edu, +1334-524-6076

Authors

Archana Bansode − *Center for Polymers and Advanced Composites, Gavin Engineering Research Laboratory, Auburn University, Auburn, Alabama 36849, United States; Department of Chemical Engineering, Ross Hall, Auburn University, Auburn, Alabama 36849, United States;* orcid.org/0000-0002-4636-0023

Lorena Alexandra Portilla Villarreal − *Forest Products Development Center, School of Forestry and Wildlife Science, Auburn University, Auburn, Alabama 36849, United States*

https://doi.org/10.1021/acsapm.3c00324
ACS Appl. Polym. Mater. 2023, 5, 4118−4126

Yuyang Wang − *Center for Polymers and Advanced Composites, Gavin Engineering Research Laboratory, Auburn University, Auburn, Alabama 36849, United States; Department of Chemical Engineering, Ross Hall, Auburn University, Auburn, Alabama 36849, United States*

Osei Asafu-Adjaye − *Forest Products Development Center, School of Forestry and Wildlife Science, Auburn University, Auburn, Alabama 36849, United States*

Brian K. Via − *Forest Products Development Center, School of Forestry and Wildlife Science, Auburn University, Auburn, Alabama 36849, United States*

Ramsis Farag − *Center for Polymers and Advanced Composites, Gavin Engineering Research Laboratory, Auburn University, Auburn, Alabama 36849, United States; Department of Chemical Engineering, Ross Hall, Auburn University, Auburn, Alabama 36849, United States*

Maria L. Auad − *Center for Polymers and Advanced Composites, Gavin Engineering Research Laboratory, Auburn University, Auburn, Alabama 36849, United States; Department of Chemical Engineering, Ross Hall, Auburn University, Auburn, Alabama 36849, United States;* orcid.org/0000-0001-6932-5645

Complete contact information is available at: https://pubs.acs.org/10.1021/acsapm.3c00324

Notes

The authors declare no competing financial interest.

■ ACKNOWLEDGMENTS

This research was supported by NSF-CREST Center for Sustainable Lightweight Materials (C-SLAM), grant number #1735971 and PrinTimber NSF EPSCoR RII Track-2 FEC # 2198099.

■ REFERENCES

(1) Aladejana, J. T.; Wu, Z.; Li, D.; Guelifack, K.; Wei, W.; Wang, X. A.; Xie, Y. Facile Approach for Glutaraldehyde Cross-Linking of PVA/Aluminophosphate Adhesives for Wood-Based Panels. *ACS Sustainable Chem. Eng.* **2019**, *7*, 18524−18533.

(2) Bandara, N.; Wu, J. Randomly Oriented Strand Board Composites from Nanoengineered Protein-Based Wood Adhesive. *ACS Sustainable Chem. Eng.* **2018**, *6*, 457−466.

(3) Pang, B.; Li, M. K.; Yang, S.; Yuan, T. Q.; Du, G. B.; Sun, R. C. Eco-Friendly Phenol-Urea-Formaldehyde Co-Condensed Resin Adhesives Accelerated by Resorcinol for Plywood Manufacturing. *ACS Omega* **2018**, *3*, 8521−8528.

(4) Rebollar, M.; Pérez, R.; Vidal, R. Comparison between Oriented Strand Boards and Other Wood-Based Panels for the Manufacture of Furniture. *Mater. Des.* **2007**, *28*, 882−888.

(5) Yang, H.; Du, G.; Li, Z.; Ran, X.; Zhou, X.; Li, T.; Gao, W.; Li, J.; Lei, H.; Yang, L. Superstrong Adhesive of Isocyanate-Free Polyurea with a Branched Structure. *ACS Appl. Polym. Mater.* **2021**, *3*, 1638−1651.

(6) Yin, H.; Zhang, E.; Zhu, Z.; Han, L.; Zheng, P.; Zeng, H.; Chen, N. Soy-Based Adhesives Functionalized with Pressure-Responsive Crosslinker Microcapsules for Enhanced Wet Adhesion. *ACS Appl. Polym. Mater.* **2021**, *3*, 1032−1041.

(7) Pizzi, A. Wood Products and Green Chemistry. In *Annals of Forest Science*; Dreyer, E., Leban, J.-M., Bolte, A., Ferretti, M., Lhotka, J. M., Shuguang, L., Eds.; Springer Nature, 2016; Vol. 73, pp 185−203.

(8) Zhang, H.; Liu, P.; Musa, S. M.; Mai, C.; Zhang, K. Dialdehyde Cellulose as a Bio-Based Robust Adhesive for Wood Bonding. *ACS Sustainable Chem. Eng.* **2019**, *7*, 10452−10459.

(9) Pizzi, A. *Phenolic Resin Adhesives*, 3rd ed.; CRC Press, 2017.

(10) Zhang, J.; Zhang, M.; Zhang, Y.; Shi, S. Q.; Zhan, X.; Li, J.; Luo, J.; Gao, Q. Improving Bond Performance and Reducing Cross-Linker Dosage for Soy Flour Adhesives Inspired by Spider Silk. *ACS Sustainable Chem. Eng.* **2021**, *9*, 168−179.

(11) Zhao, Y.; Yan, N.; Feng, M. W. Biobased Phenol Formaldehyde Resins Derived from Beetle-Infested Pine Barks - Structure and Composition. *ACS Sustainable Chem. Eng.* **2013**, *1*, 91−101.

(12) Chai, Y.; Liu, J.; Zhao, Y.; Yan, N. Characterization of Modified Phenol Formaldehyde Resole Resins Synthesized in Situ with Various Boron Compounds. *Ind. Eng. Chem. Res.* **2016**, *55*, 9840−9850.

(13) Milazzo, M.; Amoresano, A.; Pasquino, R.; Grizzuti, N.; Auriemma, F.; De Stefano, F.; Sin Xicola, A.; Iodice, V.; De Rosa, C. Curing Efficiency of Novolac-Type Phenol−Formaldehyde Resins from Viscoelastic Properties. *Macromolecules* **2021**, *54*, 11372−11383.

(14) Gao, Z.; Lang, X.; Chen, S.; Zhao, C. Mini-Review on the Synthesis of Lignin-Based Phenolic Resin. *Energy Fuels* **2021**, *35*, 18385−18395.

(15) Gustin, J. L. Vent Sizing for the Phenol + Formaldehyde Reaction. *Org. Process Res. Dev.* **2006**, *10*, 1263−1274.

(16) He, Z.; Zhang, Y.; Wei, W. Formaldehyde and VOC Emissions at Different Manufacturing Stages of Wood-Based Panels. *Build. Environ.* **2012**, *47*, 197−204.

(17) Wang, L.; Lagerquist, L.; Zhang, Y.; Koppolu, R.; Tirri, T.; Sulaeva, I.; von Schoultz, S.; Vähäsalo, L.; Pranovich, A.; Rosenau, T.; Eklund, P. C.; Willför, S.; Xu, C.; Wang, X. Tailored Thermosetting Wood Adhesive Based on Well-Defined Hardwood Lignin Fractions. *ACS Sustainable Chem. Eng.* **2020**, *8*, 13517−13526.

(18) Yao, J.; Odelius, K.; Hakkarainen, M. Microwave Hydrophobized Lignin with Antioxidant Activity for Fused Filament Fabrication. *ACS Appl. Polym. Mater.* **2021**, *3*, 3538−3548.

(19) He, Q.; Ziegler-Devin, I.; Chrusciel, L.; Obame, S. N.; Hong, L.; Lu, X.; Brosse, N. Lignin-First Integrated Steam Explosion Process for Green Wood Adhesive Application. *ACS Sustainable Chem. Eng.* **2020**, *8*, 5380−5392.

(20) Jedrzejczyk, M. A.; Kouris, P. D.; Boot, M. D.; Hensen, E. J. M.; Bernaerts, K. V. Renewable Thiol-Yne "Click" Networks Based on Propargylated Lignin for Adhesive Resin Applications. *ACS Appl. Polym. Mater.* **2022**, *4*, 2544−2552.

(21) Sun, Y. C.; Liu, X. N.; Wang, T. T.; Xue, B. L.; Sun, R. C. Green Process for Extraction of Lignin by the Microwave-Assisted Ionic Liquid Approach: Toward Biomass Biorefinery and Lignin Characterization. *ACS Sustainable Chem. Eng.* **2019**, *7*, 13062−13072.

(22) Lake, M. A.; Blackburn, J. C. SLRP - An Innovative Lignin-Recovery Technology. *Cellul. Chem. Technol.* **2014**, *48*, 799−804.

(23) Borrega, M.; Pärnilä, S.; Greca, L. G.; Jäskeläinen, A. S.; Ohra-Aho, T.; Rojas, O. J.; Tamminen, T. Morphological and Wettability Properties of Thin Coating Films Produced from Technical Lignins. *Langmuir* **2020**, *36*, 9675−9684.

(24) Çetin, N. S.; Özmen, N. Use of Organosolv Lignin in Phenol-Formaldehyde Resins for Particleboard Production: II. Particleboard Production and Properties. *Int. J. Adhes. Adhes.* **2002**, *22*, 481−486.

(25) Pizzi, A. Recent Developments in Eco-Efficient Bio-Based Adhesives for Wood Bonding: Opportunities and Issues. *J. Adhes. Sci. Technol.* **2006**, *20*, 829−846.

(26) Kouisni, L.; Fang, Y.; Paleologou, M.; Ahvazi, B.; Hawari, J.; Zhang, Y.; Wang, X. M. Kraft Lignin Recovery and Its Use in the Preparation of Lignin-Based Phenol Formaldehyde Resins for Plywood. *Cellul. Chem. Technol.* **2011**, *45*, 515−520.

(27) Solt, P.; Rößiger, B.; Konnerth, J.; van Herwijnen, H. W. G. Lignin Phenol Formaldehyde Resoles Using Base-Catalysed Depolymerized Kraft Lignin. *Polymers* **2018**, *10*, 1162.

(28) Zhang, Y.; Wu, J. Q.; Li, H.; Yuan, T. Q.; Wang, Y. Y.; Sun, R. C. Heat Treatment of Industrial Alkaline Lignin and Its Potential Application as an Adhesive for Green Wood-Lignin Composites. *ACS Sustainable Chem. Eng.* **2017**, *5*, 7269−7277.

(29) Karthäuser, J.; Biziks, V.; Mai, C.; Militz, H. Lignin and Lignin-Derived Compounds for Wood Applications—A Review. *Molecules* **2021**, *26*, 2533.

(30) Asafu-Adjaye, O. A.; Street, J.; Bansode, A.; Auad, M. L.; Peresin, M. S.; Adhikari, S.; Liles, T.; Via, B. K. Fast Pyrolysis Bio-Oil-Based Epoxy as an Adhesive in Oriented Strand Board Production. *Polymer* **2022**, *14*, 1244.
(31) Bansode, A.; Barde, M.; Asafu-Adjaye, O.; Patil, V.; Hinkle, J.; Via, B. K.; Adhikari, S.; Adamczyk, A. J.; Farag, R.; Elder, T.; Labbé, N.; Auad, M. L. Synthesis of Biobased Novolac Phenol-Formaldehyde Wood Adhesives from Biorefinery-Derived Lignocellulosic Biomass. *ACS Sustainable Chem. Eng.* **2021**, *9*, 10990−11002.
(32) Deng, S.; Du, G.; Li, X.; Pizzi, A. Performance and Reaction Mechanism of Zero Formaldehyde-Emission Urea-Glyoxal (UG) Resin. *J. Taiwan Inst. Chem. Eng.* **2014**, *45*, 2029−2038.
(33) Van Nieuwenhove, I.; Renders, T.; Lauwaert, J.; De Roo, T.; De Clercq, J.; Verberckmoes, A. Biobased Resins Using Lignin and Glyoxal. *ACS Sustainable Chem. Eng.* **2020**, *8*, 18789−18809.
(34) Liimatainen, H.; Visanko, M.; Sirviö, J. A.; Hormi, O. E. O.; Niinimaki, J. Enhancement of the Nanofibrillation of Wood Cellulose through Sequential Periodate-Chlorite Oxidation. *Biomacromolecules* **2012**, *13*, 1592−1597.
(35) Esen, E.; Meier, M. A. R. Sustainable Functionalization of 2,3-Dialdehyde Cellulose via the Passerini Three-Component Reaction. *ACS Sustainable Chem. Eng.* **2020**, *8*, 15755−15760.
(36) Chen, X.; Xi, X.; Pizzi, A.; Fredon, E.; Du, G.; Gerardin, C.; Amirou, S. Oxidized Demethylated Lignin as a Bio-Based Adhesive for Wood Bonding. *J. Adhes.* **2021**, *97*, 873−890.
(37) Zhang, Y.; Fatehi, P. Periodate Oxidation of Carbohydrate-Enriched Hydrolysis Lignin and Its Application as Coagulant for Aluminum Oxide Suspension. *Ind. Crops Prod.* **2019**, *130*, 81−95.
(38) Gosselink, R. J. A.; Van Dam, J. E. G.; De Jong, E.; Gellerstedt, G.; Scott, E. L.; Sanders, J. P. M. Effect of Periodate on Lignin for Wood Adhesive Application. *Holzforschung* **2011**, *65*, 155−162.
(39) Tummalapalli, M.; Gupta, B. A UV-Vis Spectrophotometric Method for the Estimation of Aldehyde Groups in Periodate-Oxidized Polysaccharides Using 2,4-Dinitrophenyl Hydrazine. *J. Carbohydr. Chem.* **2015**, *34*, 338−348.
(40) Kandrac, M. *Factors Affecting the 2,4-Dinitrophenyl Hydrazine Reaction With Lipid Carbonyls*; Rutgers University, 2018.
(41) Shannon, S. K.; Barany, G. Colorimetric Monitoring of Solid-Phase Aldehydes Using 2,4- Dinitrophenylhydrazine. *J. Comb. Chem.* **2004**, *6*, 165−170.
(42) Knicker, H.; Velasco-Molina, M.; Knicker, M. 2D Solid-State Hetcor1H-13C Nmr Experiments With Variable Cross Polarization Times As a Tool for a Better Understanding of the Chemistry of Cellulose-Based Pyrochars—a Tutorial. *Appl. Sci.* **2021**, *11*, 8569.
(43) Le Brech, Y.; Delmotte, L.; Raya, J.; Brosse, N.; Gadiou, R.; Dufour, A. High Resolution Solid State 2D NMR Analysis of Biomass and Biochar. *Anal. Chem.* **2015**, *87*, 843−847.
(44) Cao, X.; Drosos, M.; Leenheer, J. A.; Mao, J. Secondary Structures in a Freeze-Dried Lignite Humic Acid Fraction Caused by Hydrogen-Bonding of Acidic Protons with Aromatic Rings. *Environ. Sci. Technol.* **2016**, *50*, 1663−1669.
(45) Chen, S.; Xin, Y.; Zhao, C. Multispectroscopic Analysis in the Synthesis of Lignin-Based Biophenolic Resins. *ACS Sustainable Chem. Eng.* **2021**, *9*, 15653−15660.
(46) Siahkamari, M.; Emmanuel, S.; Hodge, D. B.; Nejad, M. Lignin-Glyoxal: A Fully Biobased Formaldehyde-Free Wood Adhesive for Interior Engineered Wood Products. *ACS Sustainable Chem. Eng.* **2022**, *10*, 3430−3441.

https://doi.org/10.1021/acsapm.3c00324
ACS Appl. Polym. Mater. 2023, 5, 4118−4126